Oncogene
https://doi.org/10.1038/s41388-018-0654-9

ARTICLE

Spironolactone inhibits the growth of cancer stem cells by impairing DNA damage response

Ayala Gold[1] · Lital Eini[1] · Malka Nissim-Rafinia[1,2] · Ruth Viner[1] · Shlomit Ezer[1] · Keren Erez[1] · Nasma Aqaqe[3] · Rotem Hanania[1] · Michael Milyavsky[3] · Eran Meshorer[1,2] · Michal Goldberg[1]

Received: 10 June 2018 / Revised: 30 October 2018 / Accepted: 7 December 2018

Abstract

The cancer stem cell (CSC) model suggests that a subpopulation of cells within the tumor, the CSCs, is responsible for cancer relapse and metastasis formation. CSCs hold unique characteristics, such as self-renewal, differentiation abilities, and resistance to chemotherapy, raising the need for discovering drugs that target CSCs. Previously we have found that the antihypertensive drug spironolactone impairs DNA damage response in cancer cells. Here we show that spironolactone, apart from inhibiting cancerous cell growth, is also highly toxic to CSCs. Notably, we demonstrate that CSCs have high basal levels of DNA double-strand breaks (DSBs). Mechanistically, we reveal that spironolactone does not damage the DNA but impairs DSB repair and induces apoptosis in cancer cells and CSCs while sparing healthy cells. In vivo, spironolactone treatment reduced the size and CSC content of tumors. Overall, we suggest spironolactone as an anticancer reagent, toxic to both cancer cells and, particularly to, CSCs.

Introduction

Cancer is the second most common cause of death in US, accounting for nearly one in every four deaths. Although tremendous efforts are being invested in the detection, prevention and treatment of cancer, the numbers of morbidity and mortality are still rising [1]. An enabling characteristic of cancer cells is genomic instability [2], which may arise from different insults, including telomere damage, centrosome amplification, and DNA damage [3]. Radiation, as well as a large fraction of chemotherapeutic agents, are used for the sole purpose of inflicting severe damage to the DNA. DNA damage response (DDR) is a natural pathway evolved by cells to repair DNA and maintain genomic stability. The response includes sensing a wide variety of damage to DNA, signaling and repairing the damage if possible. In cases of failure to repair the damage, alternative outcomes are available, such as apoptosis or senescence [4]. The concept of aiming at DNA as a target for anticancer drugs inspired the development of numerous anticancer compounds. Combining the treatment of DNA-damaging agents with inhibitors of DNA-repair pathways, therefore, has the potential to sensitize cells to DNA-damaging agents [5].

A few years ago, we [6] and others [7, 8] found that spironolactone reduces frequencies of DNA repair in cancer cells as well as affects the growth of cancer cells and sensitizes them to chemotherapy. Spironolactone is an aldosterone antagonist drug approved by the Food and Drug Administration used in the clinic primarily for treating high blood pressure and heart failure conditions [9, 10]. We showed that spironolactone inhibits human osteosarcoma U2OS cell growth by interfering with DNA double-strand break (DSB) repair by homologous recombination [6].

Supplementary information The online version of this article (https://doi.org/10.1038/s41388-018-0654-9) contains supplementary material, which is available to authorized users.

✉ Eran Meshorer
eran.meshorer@mail.huji.ac.il

✉ Michal Goldberg
goldbergm@mail.huji.ac.il

[1] Department of Genetics, The Institute of Life Sciences, The Hebrew University of Jerusalem, Edmond J. Safra Campus, Givat Ram, Jerusalem 9190401, Israel

[2] The Edmond and Lily Safra Center for Brain Sciences (ELSC), The Hebrew University of Jerusalem, Edmond J. Safra Campus, Givat Ram, Jerusalem 9190401, Israel

[3] Department of Pathology, Sackler Faculty of Medicine, Tel-Aviv University, Tel-Aviv 69978, Israel

Published online: 08 January 2019

Spironolactone was also demonstrated to sensitize human cervical carcinoma HeLa cells to platinum derivatives by promoting degradation of the xeroderma pigmentosum type-B subunit of the transcription/repair factor TFIIH (transcription factor II human), which plays a key role in nucleotide excision repair [7]. In colon cancer cell lines, spironolactone upregulates the expression of a group of major histocompatibility complex class I-like molecules, the NKG2D ligands, by activating the ATM-Chk2-mediated checkpoint pathway independent of DNA damage induction. Spironolactone enhances tumor elimination by natural killer cells, via retinoid X receptor-γ activation [8].

Combination treatments using DNA-damaging chemotherapeutic agents, together with molecules that impair DNA repair, can significantly prolong the survival of cancer patients, but unfortunately do not guarantee long-term cancer prevention. In many cases, a relapse of cancer occurs months or even years after apparently successful treatments [11]. A partial elimination of tumor growth and treatment failure in the long run can be attributed, at least in part, to the presence of cancer stem cells (CSCs) in the tumor [12, 13]. According to the CSC model, only a subset of cancer cells, the CSCs, display stem cell properties, including self-renewal and the capacity to differentiate. Although the CSC population usually comprises less than 1% of the total cells within the tumor [12], it is this group of cells that initiate tumors and are considered the major reason for relapse, resistance to therapies, and metastasis [14, 15]. The low abundance of CSCs in tumors raised the need for the development of different CSC systems, which offers different experimental and conceptual advantages. Examples are the CSC-like (CSCL) and the stem-like glioma cell (SLGC) systems [16, 17]. The CSCL cells were generated by transforming human differentiated fibroblasts in vitro. These transformed cells were able to initiate tumors when injected into immunocompromised mice. CSCL cells were isolated from these tumors as a subpopulation of cells reprogrammed to a more primitive, multipotent cell type that present the stage-specific early antigen-1 (SSEA1) surface marker. These CSCL cells possess hallmarks of CSCs, such as the ability to self-renew, differentiate along several lineages, and initiate and maintain hierarchically organized tumors [16]. This CSC model system enables to characterize the common features of CSCs and compare them with control cells [18]. The SLGC system is comprised of cells derived from glioblastomas [17]. The SLGCs were isolated as a $CD133^+$ cell subpopulation from human brain tumors, and they grow as floating, dense cell aggregates termed neurospheres [19] and display stem-cell properties in vitro, as well as in vivo, as measured by their capacity to self-renew and recapitulate the original tumor properties [17].

In order to characterize spironolactone as a potential drug in cancer treatment, crucial knowledge was lacking both in terms of spironolactone safety to healthy cells on the one hand and its ability to affect CSCs on the other hand. Since CSCs play a crucial role in tumor formation, maintenance, and metastasis, it is essential to specifically understand the effect of spironolactone on molecular processes such as DDR and on CSC growth in vitro and in vivo.

Here we report that spironolactone does not induce DNA damage, but rather impairs DNA repair in cancer as well as in CSCs and spares healthy cells. Notably, spironolactone is toxic to both CSCLs and SLGCs while is safe for healthy cells. Moreover, in mice, spironolactone was able to slow down tumor growth and, remarkably, reduce CSC content in the tumors.

Results

Spironolactone inhibits the growth of cancer cells but not of healthy cells

We and others found that spironolactone is toxic to cancer cells [6–8]. We first aimed to broaden our understanding of the effect of spironolactone on cancer cells and to examine whether it is toxic to non-cancerous healthy cells. To this end, U2OS (bone epithelial cells derived from osteosarcoma) or HeLa (cervix epithelial cancer cells derived from adenocarcinoma) cells were treated for one hour with growing concentrations of spironolactone or with dimethyl sulfoxide (DMSO) as a control. Where indicated, the radiomimetic agent phleomycin, which induces DNA damage and thus mimics the effect of chemotherapy in the clinic, was added for an hour, then the cells were washed to remove phleomycin and allowed to recover for 96 h in the presence of spironolactone or DMSO. U2OS and HeLa cancer cells treated with phleomycin alone displayed growth inhibition of about 40 and 80%, respectively, compared to the control (DMSO) treatment (Fig. 1a and Supplementary Fig. S1A; gray lines). Spironolactone treatment alone affected cell growth in a dose-dependent manner in both U2OS and HeLa cell lines (Fig. 1a and Supplementary Fig. S1A). The highest concentration tested for spironolactone (50 μM) resulted in about 80 or 90% growth inhibition in U2OS or HeLa cells, respectively. Inducing DNA damage by phleomycin in the spironolactone-treated cancer cells had a slightly larger effect on growth inhibition than each of the treatments alone (Fig. 1 and Supplementary Fig. S1A). To further test the additive effect of DNA-damage induction combined with spironolactone, U2OS cells were treated with the DNA-damaging chemotherapeutic agent, cisplatin. As expected,

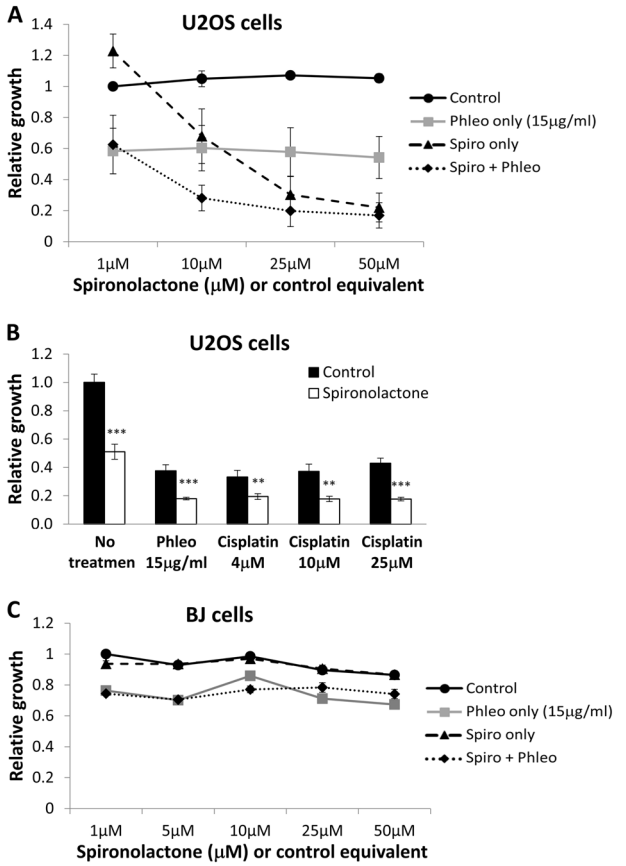

Fig. 1 Spironolactone inhibits the growth of cancer cells but not of healthy cells. U2OS (**a**, **b**) or BJ (**c**) cells were treated with the indicated concentrations of spironolactone (Spiro; **a**, **c**), with 25 μM spironolactone (**b**), or with equivalent volumes of DMSO (Control) for 1 h prior to 1 h treatment with phleomycin (**a**–**c**) or cisplatin at the indicated concentrations (**b**). Cells recovered in the absence of phleomycin or cisplatin in an appropriate fresh medium containing DMSO or spironolactone at the indicated concentrations for 96 h. Cells were fixed and stained with methylene blue. Relative growth was quantified by reading at 620 nm in a microplate reader. Values were normalized to the lowest control amount and are shown as the average of three experiments, six technical repeats each (**a**, **c**) or an average of 3–6 technical repeats of a representative experiment (**b**). SE bars are shown

treating U2OS cells with either one of the DNA-damaging agents resulted in the inhibition of the relative growth of the cells (Fig. 1b; compare Control bar of no treatment to Control bars of cells treated with phleomycin or cisplatin). Addition of spironolactone to the cells resulted in about 50% growth inhibition compared to the control in non-treated cells as well as in cells treated with both DNA-damaging agents and spironolactone (Fig. 1b; compare Control to Spiro bars in each treatment).

To assess the safety of spironolactone use for therapy it was important to check the effect of spironolactone on the ability of healthy, non-cancerous cells to grow. Cell lines derived from healthy tissues (foreskin BJ cells, the immortalized foreskin cell lines BJ and FSE (BJ hTERT and FSE hTERT, respectively) and the immortalized retinal pigment epithelial cells (RPE1 hTERT)) were treated as described above for the cancer cells. Treating the healthy cells with phleomycin resulted in a diverse inhibition of cell growth, from about 20% inhibition in BJ fibroblast cells (Fig. 1c; Phleo line) to about 40% inhibition in BJ hTERT and FSE hTERT cells (Supplementary Fig. 1B, C; Phleo lines) and up to about 80% growth inhibition in RPE1 hTERT cells (Supplementary Fig. 1d; Phleo line). Notably, the treatment of these healthy cells with spironolactone had either no effect on growth (Fig. 1c; circles) or a small inhibiting effect at high concentrations of 25–50 μM (Supplementary Fig. S1B–D; Spiro lines). This inhibition is to a lesser extent than the parallel phleomycin treatment (Supplementary Fig. S1B–D; compare Phleo lines to Spiro lines). Combining the treatment of phleomycin with recovery in the presence of spironolactone did not cause an additional growth inhibition when compared to phleomycin alone, in all the cases (Fig. 1c and Supplementary Fig. S1B–D; compare Spiro + Phleo lines to Phleo lines). These results suggest that spironolactone does not add toxicity to the healthy cells already treated with a DNA-damaging chemotherapeutic agent.

Spironolactone inhibits the growth of chemoresistant cancer stem cells

In view of the ability of spironolactone to inhibit the growth of cancer cells treated with DNA-damaging agents, we were interested to examine the specific effect of spironolactone on CSC subpopulation. This is extremely important since CSCs are resistant to most conventional treatments. We started out by testing the response to chemotherapy of in vitro generated CSCs (CSCL cells) [16]. These cells were generated by the immortalization and transformation of human fibroblast cells and were selected for the embryonic stem cell marker SSEA1. These cells have properties of CSCs, such as self-renewal and the ability to generate hierarchically organized tumors [16] (Fig. 2a). As expected from CSCs, CSCL cells, in contrast to U2OS cells, display resistance to the DNA-damaging agent phleomycin (Fig. 2b; compare no treatment to Phleo bars and Fig. 2c; compare Control to Phleo lines), as well as to growing concentrations of the chemotherapeutic agent cisplatin (Fig. 2b). Only the highest cisplatin concentration used (25 μM) resulted in a slight growth reduction of CSCL cells (32%), while a low cisplatin concentration of 4 μM was sufficient to inhibit U2OS cell growth by 67% (Fig. 2b). As opposed to phleomycin and cisplatin treatments, the addition of spironolactone to the CSCL cells resulted in a marked growth inhibition of up to 80% compared to the control treatment (Fig. 2c; Spiro line). The growth inhibition of the CSCL cells by spironolactone was not influenced by any prior treatment with phleomycin (Fig. 2c; Spiro + Phleo line), which is not surprising since

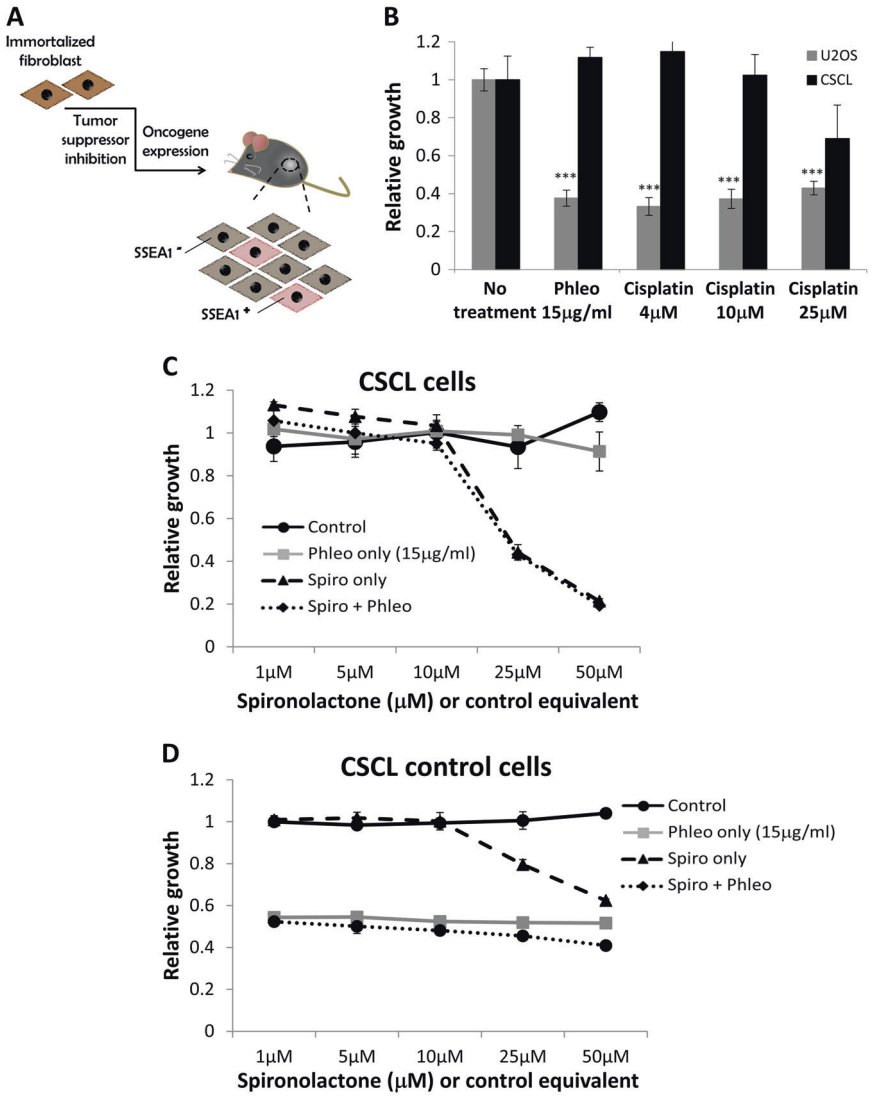

Fig. 2 Spironolactone inhibits the growth of chemoresistant cancer stem cell-like (CSCL) cells. **a** CSCL model system: human immortalized (hTERT) fibroblasts were transformed in vitro through the expression of the oncogenic H-RasV12 mutant, along with the inhibition of p53 and pRB tumor suppressor pathways (by expressing simian virus 40 large and small T antigens). The transformed cells are able to initiate tumors when injected into immunocompromised mice, and a subpopulation of cells reprogram to a more primitive, multipotent cell type that presents the stage-specific early antigen-1 (SSEA1) surface marker. These CSCL cells possess hallmarks of CSCs, such as the ability to self-renew, to differentiate along several lineages, and to initiate and maintain hierarchically organized tumors. **b** U20S and CSCL cells were treated with either phleomycin or the indicated cisplatin concentrations for 1 h. The cells were then allowed to recover in a fresh medium for 96 h. CSCL (**c**) or CSCL control cells (original immortalized fibroblasts) (**d**) were treated with the indicated concentrations of spironolactone or DMSO (Control) for 1 h prior to the treatment with phleomycin. Cells recovered in the fresh medium containing spironolactone or DMSO at the indicated concentrations, for 96 h. Cells were fixed and stained with methylene blue. Relative growth was quantified by reading at 620 nm in a microplate reader. Values were normalized to the lowest control amount and are shown as the average of three experiments, six technical repeats each (**c**, **d**) or normalized to control and shown as the average of 3–6 technical repeats of a representative experiment (**b**). SE bars are shown

the CSCL cells display resistance to phleomycin treatment (Fig. 2b, c; Phleo bar and line, respectively). The original immortalized fibroblasts, which did not undergo transformation, served as a control for the CSCL cells. Importantly, the growth of these control cells was inhibited to about 50% by phleomycin (Fig. 2d; Phleo line). Spironolactone inhibited the growth of the control cells to a lesser extent compared to the CSCL cells. Treating cells with 25 and 50 µM spironolactone resulted in a growth inhibition, compared to control, of 67 and 81%, respectively, in CSCL cells, while in the control cells the reduction was of 40 and 38%, respectively (Fig. 2d; Spiro line). Moreover, the effect of spironolactone on growth inhibition of the control cells was smaller than the effect of phleomycin on the cells (Fig. 2d;

compare Spiro line to Phleo line: treatment with 25 and 50 μM spironolactone resulted in a relative growth inhibition of 40 and 38%, respectively, compared to about 50% growth inhibition upon phleomycin treatment). A combined treatment of spironolactone (50 μM) and phleomycin resulted in a growth inhibition that was slightly higher than phleomycin alone (Fig. 2d; compare Spiro + Phleo and Phleo lines: an inhibition of up to 59% in the combined treatment compared to 48% inhibition with phleomycin alone). Taken together, our results suggest that CSCL control cells are less sensitive to spironolactone compared to cancer cells and CSCL cells (compare Fig. 2d to Fig. 1a–c and Supplementary Fig. S1A), but are more sensitive to spironolactone compared to healthy cells (compare Fig. 2d to Fig. 1c and Supplementary Fig. 1B–D).

The dramatic effect of spironolactone on CSCs was further examined in an additional CSC system, the SLGCs. SLGCs comprise a subpopulation of glioblastoma tumor cells capable of differentiating into the actively expanding tumor, and they grow as floating, dense cell aggregates termed neurospheres [19], a typical state of normal neural stem cells (Supplementary Fig. 2A). Loss of neurosphere-like shape is a phenomenon well-known from differentiating neuronal stem cells and is correlated with the loss of stemness properties [20]. Treating cells with control (DMSO) or phleomycin did not affect neurosphere state; the spheres persist in an aggregate form of normal size (Supplementary Fig. 2B). The observed resistance to phleomycin treatment in SLGCs was the strikingly opposite to the effect of spironolactone on these cells; when cells were treated with spironolactone in growing concentrations, a shift in neurosphere state was observed as the spheres grew smaller in a dose-dependent manner (Supplementary Fig. 2B). Small neurospheres can indicate either the loss of stemness traits which enable aggregation, while retaining the ability to divide, or can be due to an overall growth inhibition and cell death. To determine which of the above options is the actual consequence of spironolactone treatment, we also assessed the cells' viability. SLGC growth was inhibited by 81% following spironolactone treatment (Supplementary Fig. 2C), which is similar to the effect of spironolactone on the CSCL cells (Fig. 2b). Combining spironolactone with phleomycin did not inhibit the growth of the SLGCs more than spironolactone treatment alone (compare Supplementary Fig. 2D Spiro vs Spiro + Phleo). In both cases, growth was inhibited to about 50% of the effect of phleomycin alone, indicating that the major cause of growth inhibition was the spironolactone treatment.

CSCs display traits that are derived both from stemness and their cancerous nature. It was important to determine whether the strong effect of spironolactone on CSC growth was merely a result of their stemness, in which case it may be dangerous to treat patients with spironolactone. To determine the effect of spironolactone on stem cells we monitored the ability of human hematopoietic stem and progenitor cells (HSPCs) to form colonies in the presence of spironolactone. Since spironolactone treatment is proposed to be combined with chemotherapy, we tested the effect of phleomycin treatment, which is known to be quite toxic [21], with or without spironolactone treatment, on HSPCs. A continuous exposure to low concentrations of spironolactone (1 μM) yields a similar number of colonies as the control alone. Higher concentrations of spironolactone result in a gradual decrease in the number of colonies. In contrast, 1 h incubation with phleomycin led to a sixfold decrease in HSPC colony formation (Supplementary Fig. S2E). It is worthy of note that spironolactone did not alter the cytotoxic potential of phleomycin (Supplementary Fig. S2E). Also, spironolactone did not change the differentiation potential of HSPCs, as a similar fraction of erythroid, monocyte, and granulocyte colonies were scored in spironolactone and DMSO treatments (data not shown). These results reveal that normal human HSCPs are not more sensitive to spironolactone than phleomycin treatments.

Spironolactone impairs DNA repair in cancer and cancer stem cells but not in healthy cells

To uncover the basis of the differential effect of spironolactone on the growth of healthy, cancer and CSCs, we examined whether this is due to changes in the inhibitory effect of spironolactone on DNA repair in the different cell types. First, we proceeded to evaluate the ability of cells to repair DSBs in the presence of spironolactone in an attempt to understand the differential response of the distinct cell types to spironolactone treatment. One of the first stages of cellular response to DNA damage is the sensing and marking of the site of damage to enable the recruitment of mediators and effectors to the break site. Phosphorylation of the histone variant H2AX (γH2AX) is a well-known marker for DSB formation. Dephosphorylation of γH2AX indicates that the break has been processed and repaired. To assess the effect of spironolactone on the response to DNA damage we induced DNA damage by phleomycin and then allowed the cells to recover for 6 h in the presence of spironolactone to allow repair to take place. Antibodies directed against γH2AX were used to recognize the break sites, and those microscopic foci were viewed under a fluorescent microscope (Fig. 3a, b). Treating cells with the DNA-damaging agent phleomycin caused, as expected, an elevation in the average number of foci per cell in healthy cells (BJ hTERT: Fig. 3a; gray bars and 3b; 'Phleo') and in cancer cells (U2OS: Fig. 3a; black bars and 3b; 'Phleo'). Focus formation by γH2AX in CSCs (CSCL cells), on the other hand, did not show any difference between cells treated with phleomycin and control (Fig. 3a; striped bars

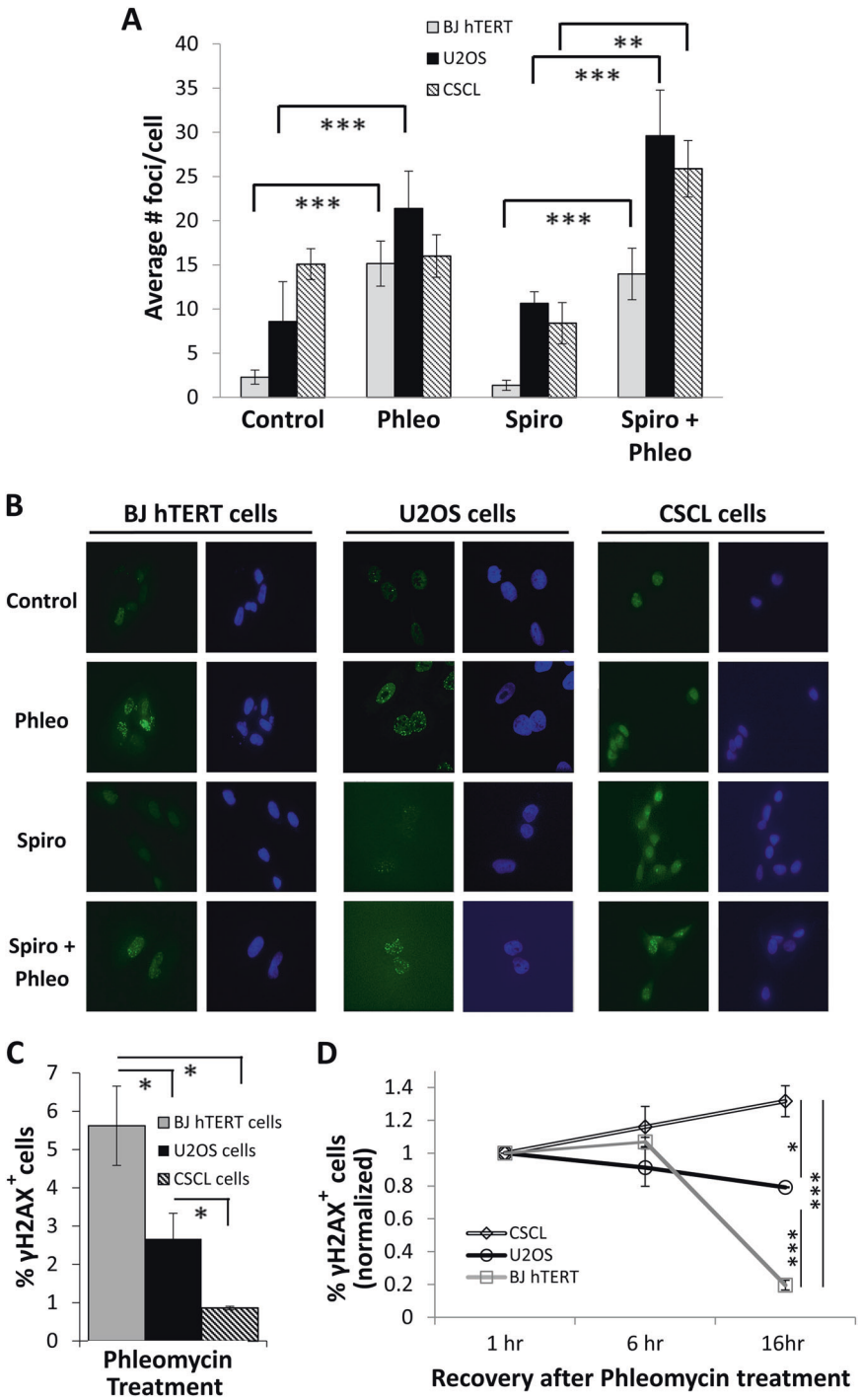

Fig. 3 Spironolactone affects DNA damage response in cancer and cancer stem cell-like (CSCL) cells but not in healthy cells. BJ hTERT, U2OS and CSCL cells were treated with 40 μM spironolactone (Spiro) or DMSO (Control) for 1 h followed by phleomycin treatment (10 μg/ml, 1 h) for DSB induction where indicated. Cells were allowed to recover for 6 h in the presence or absence of spironolactone. Cells were immunostained with an anti-γH2AX antibody and DAPI. Results are shown as the average number of foci per cell with at least 50 cells analyzed for each treatment (**a**) or representative images (**b**). **c, d** BJ hTERT, U2OS, and CSCL cells were treated with DMSO (**c**) or with 40 μM spironolactone or DMSO as a control (**d**) for 1 h prior to the addition of phleomycin (15 μg/ml, 1 h). Cells were then collected (**c**) or allowed to recover for the indicated times in appropriate media before being collected (**d**). Cells were fixed and stained with an anti-γH2AX antibody. Percent of $\gamma H2AX^{+}$ cells was determined by flow cytometry. Thirty thousand cells were analyzed for each experiment. Results are shown as the average of 2–3 repeats (**c**, **d**). Significance was calculated by a two-tailed *t* test. Values were normalized to elevation from control treatment (**c**) or to elevation from spironolactone treatment (**d**) and set as 1

and 3B; 'Phleo'), once again displaying chemoresistance. Treating all types of cells with spironolactone alone did not cause the accumulation of foci in all cell types (Fig. 3a, b; 'Spiro'). In contrast, the combination of spironolactone and phleomycin treatments showed a trend of elevation in average foci number in cells, both in U2OS and CSCL cells but not in BJ hTERT cells (Fig. 3a, b; 'Spiro + Phleo'). This indicates that spironolactone addition to cancer cells and CSCs, but not to healthy cells, impairs DNA repair. To further investigate the differential effect of spironolactone on DNA repair in different cell types, we followed the levels of γH2AX in additional time points and over thousands of cells by quantifying γH2AX signal using flow cytometry. Analyzing the levels of γH2AX at different time points after DNA-damage induction indicates the progress of the repair process. Under normal conditions, the levels of γH2AX in untreated cells is expected to be low. Early upon DSB induction, the level should rise and then decrease with

time, as DNA repair occurs. As expected, treating U2OS and BJ hTERT cells with phleomycin for 1 h resulted in an elevation of γH2AX levels (Fig. 3c and Supplementary Fig. S3A,C). In contrast, when CSCL cells were treated with phleomycin no elevation in γH2AX levels was detected (Fig. 3c and Supplementary Fig. S3E), which is in line with our previous observation of resistance of the CSCL cells to phleomycin (Fig. 2b, c). γH2AX levels in BJ hTERT cells treated with phleomycin and left to recover for 16 h dropped back to normal levels (Supplementary Fig. S3A), indicating that the DNA was repaired by 16 h in these cells. In U2OS cells, the repair was attenuated; γH2AX levels 16 h after phleomycin treatment were reduced although they did not return to control levels (Supplementary Fig. S3C). As expected, since the addition of phleomycin to CSCL cells did not affect γH2AX levels, there was no reduction 16 h after phleomycin addition (Supplementary Fig. S3E). Next, we analyzed DSB repair in the presence of spironolactone. Addition of spironolactone in combination with DNA-damage induction had hardly no effect on BJ hTERT cells (Fig. 3d and Supplementary Fig. S3A, B). U2OS cells displayed a delayed repair in the presence of spironolactone as reflected by the relatively higher levels of γH2AX after 16 h in cells treated with phleomycin and spironolactone compared to phleomycin only (Fig. 3d and Supplementary Fig. S3C, D). Notably, in CSCL cells, γH2AX levels were slightly elevated due to the addition of spironolactone (Fig. 3d and Supplementary Fig. S3E, F).

Spironolactone does not induce DNA damage in cancer or cancer stem cells

We found that γH2AX levels in CSCs are elevated when spironolactone is added to phleomycin treatment (Fig. 3d and Supplementary Fig. S3E, F; 16 h time point), which suggests impairments in DSB repair. We wanted to verify that spironolactone does not induce DNA damage, as suggested from our observation that the addition of spironolactone does not affect γH2AX focus formation and levels in all cell types analyzed (Fig. 3a, b and Supplementary Fig. S3A, C, E). In order to exclude the possibility that spironolactone is the actual cause for DNA damage in cancer and CSCs, we evaluated DNA-damage occurrence using the comet assay. Cells were treated with spironolactone or phleomycin (as a DNA-damaging agent control) and intactness of DNA in the nuclei was measured by the length of the "tail" that was formed when applying an electrical field on lysed nuclei embedded in soft agar. Treating cells with phleomycin induced DNA damage as expected in U2OS cancer cells (Fig. 4a, b). Notably, phleomycin did not induce DNA damage in CSCL cells (Fig. 4a, b). This observation is in line with our described results of CSCL cells being resistant to phleomycin (Fig. 2b, c). A common mechanism of CSCs to resist therapy is by actively pumping the drug out of the cell by multidrug transporters. To ensure the assay was intact and CSCL cells suffering DNA damage can be detected, we treated the cells with ultra violet (UV) irradiation rather than a chemical drug such as phleomycin. When UV irradiation was applied, the recovery time was longer compared to when phleomycin was added in order to allow DSB formation from unrepaired Thymidine dimers (4 and 1 h, respectively). However, time difference in the recovery period in the presence of spironolactone did not result in difference in tail length (Supplementary Fig. S3G). UV irradiation indeed causes DNA damage both to U2OS and CSCL cells as seen by the formation of comet tails (Fig. 4b and Fig. 4c, d; lane 1 vs 3). When cells were treated with spironolactone alone, no significant tail formation was detected compared to control treatment, both in U2OS (Fig. 4c; lane 1 vs 4) and CSCL cells (Fig. 4d; lane 1 vs 4), suggesting that spironolactone does not cause damage to DNA in those cell types. Combining treatment of phleomycin and spironolactone did not cause any additional damage to the phleomycin-induced damage in both U20S (Fig. 4c; lane 2 vs 5) and CSCL cells (Fig. 4d; lane 2 vs 5). Interestingly, UV treatment combined with spironolactone caused a significant increase in DNA damage compared to UV treatment alone in U2OS cells (Fig. 4c; lane 3 vs 6). It is possible that this reflects the inhibitory effect of spironolactone on nucleotide excision repair [7], resulting in lack of repair of the Thymidine dimers induced by the UV irradiation. This increase in DNA damage seen in U2OS cells treated with both UV and spironolactone is not detected in CSCL cells (Fig. 4d; lane 3 vs 6). Taken together, these results show that spironolactone treatment of cancer cells and CSCs does not inflict direct damage to DNA. When comparing the natural state of the U2OS and CSCL cells in terms of DNA damage we came upon an interesting observation; CSCL cells displayed a significantly higher basal level of DNA damage than the cancer cells (Fig. 4a, b; compare U2OS and CSCL controls).

Spironolactone does not act through aldosterone antagonism and induces apoptosis in cancer and CSCs

Spironolactone is a widely used non-selective mineralocorticoid receptor (MR) antagonist. To reveal whether the toxicity of spironolactone to CSCs acts through antagonism to MR we took advantage of another available MR antagonist drug, eplerenone. Since eplerenone acts in a manner similar to spironolactone, but has a slightly lower affinity to the receptor, we treated CSCL cells with eplerenone in concentrations equal to and higher than spironolactone and tested whether eplerenone treatment inhibits

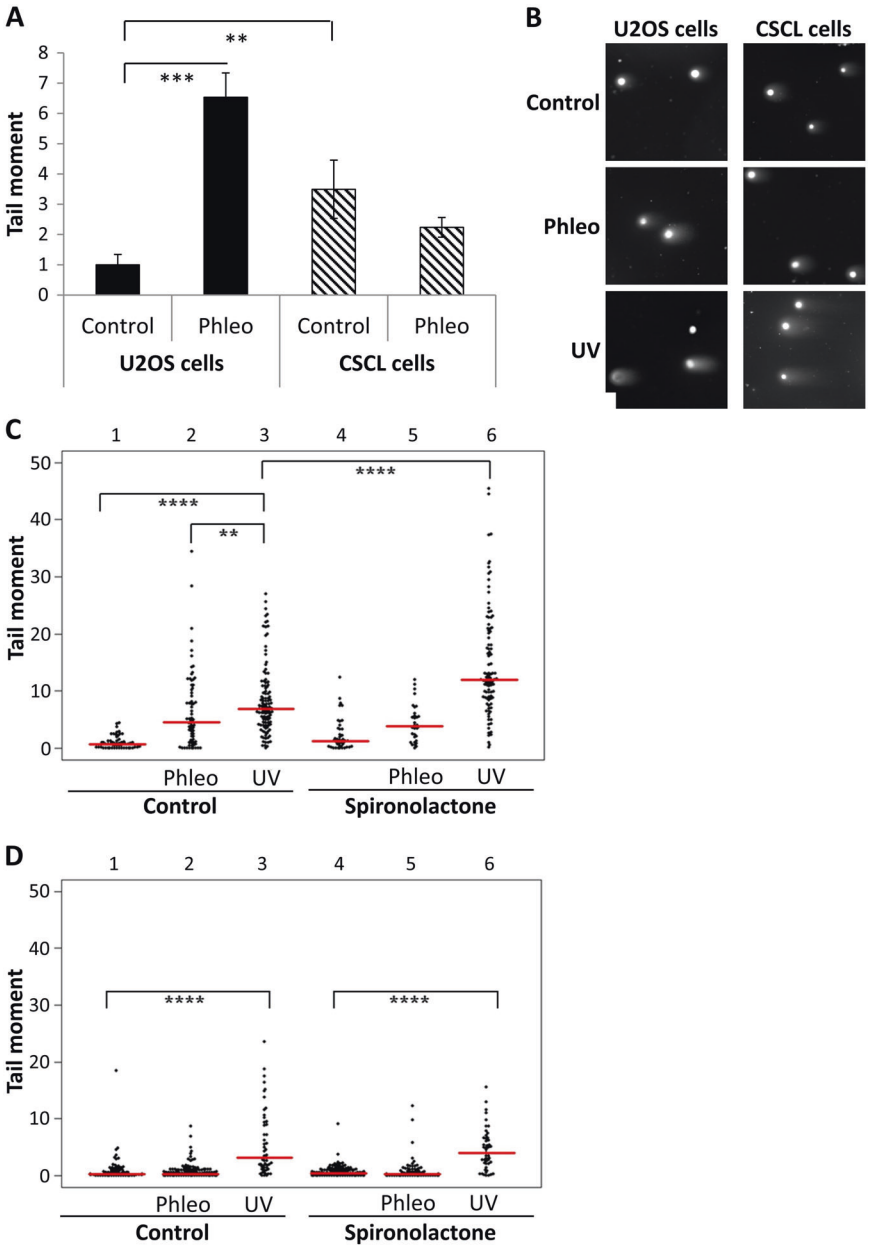

Fig. 4 Spironolactone does not induce DNA damage in cancer or cancer stem cells. **a** Differential response to phleomycin treatment (Phleo, 10 µg/ml, 1 h) in U2OS and CSCL cells. Representative images are shown in (**b**). U2OS (**c**) or CSCL (**d**) cells were treated with 40 µM spironolactone (Spiro) or DMSO (Control) for 1 h. Damage was introduced by phleomycin treatment (10 µg/ml, 1 h) or UV irradiation (4 h recovery). All cells were fixed and lysed in soft agar on glass slips, run in neutral electrophoresis conditions and stained with DAPI. Comet tails were imaged under a fluorescence microscope and analyzed with the "Open Comet" software. Values were obtained from 70–100 cells for each condition. (A, average; C, D, median). Representative images are shown in (**b**). Significance was calculated by R software

cell growth in a manner similar to spironolactone. Eplerenone treatment did not cause any growth inhibition to CSCL cells (Fig. 5a), even at a high concentration of 100 µM, which is four times higher than the concentration in which spironolactone had affected those cells originally (Supplementary Fig. S4A). This result demonstrated that spironolactone most probably does not act on cell growth through its canonical role as an MR antagonist. Treating the cells with phleomycin in the presence of eplerenone also had not caused any growth impairment (Fig. 5a). To verify that eplerenone is in fact acting as an MR antagonist in our cell system, we quantified the expression of GADD45β, a gene that was documented to be downregulated by spironolactone and eplerenone [22]. Indeed, GADD45β was downregulated by 33 or 47% after treatment with eplerenone or spironolactone, respectively (Fig. 5b), demonstrating that eplerenone activity was intact.

As the known mechanism of spironolactone could not explain the effect on cell growth, we took a more general approach to uncover the possible mechanism through which spironolactone affects cell growth. We utilized the online available bioinformatics Connectivity Map tool (CMap), which was developed to facilitate the discovery of pathways perturbed by small molecules of unknown activity, based on the common gene expression changes that similar small molecules confer [23]. Spironolactone

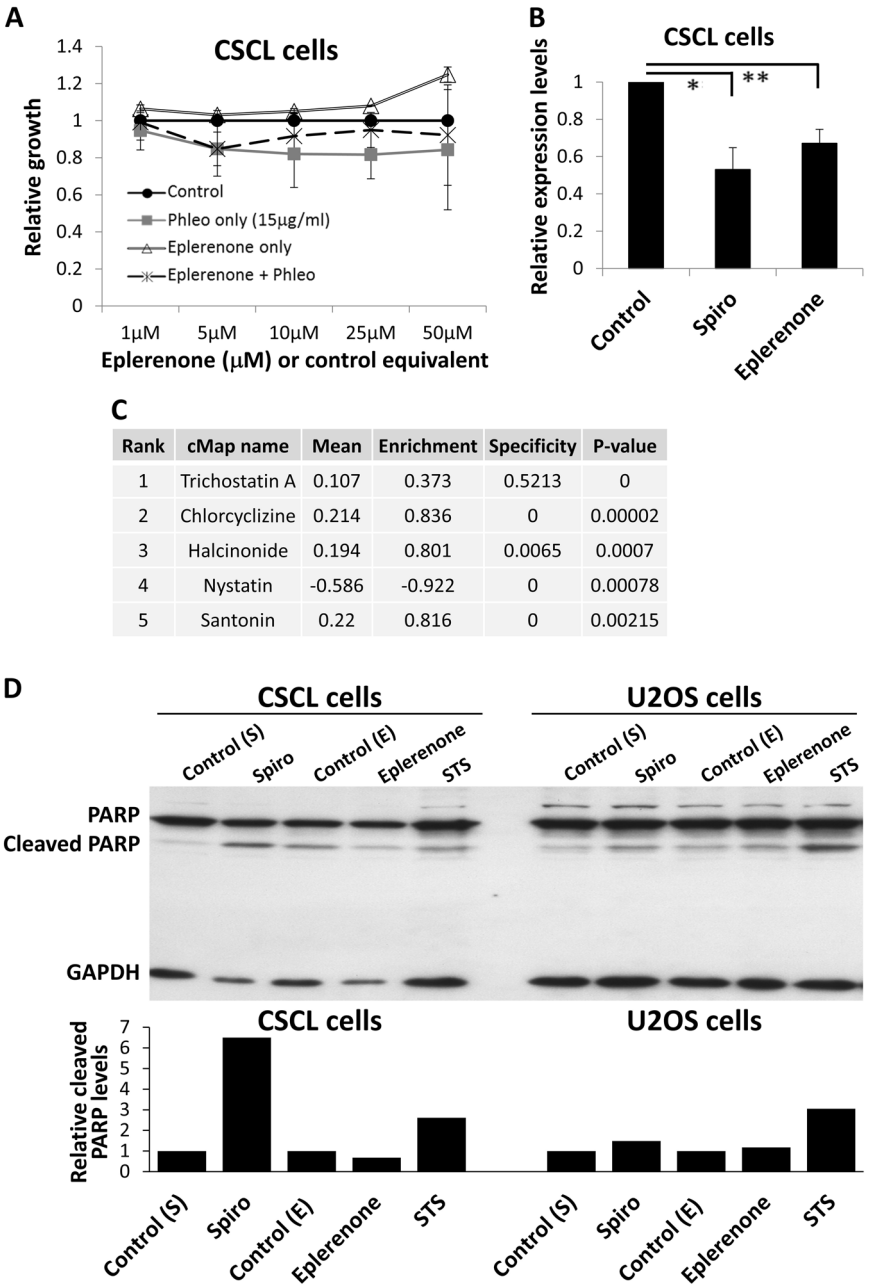

C

Rank	cMap name	Mean	Enrichment	Specificity	P-value
1	Trichostatin A	0.107	0.373	0.5213	0
2	Chlorcyclizine	0.214	0.836	0	0.00002
3	Halcinonide	0.194	0.801	0.0065	0.0007
4	Nystatin	-0.586	-0.922	0	0.00078
5	Santonin	0.22	0.816	0	0.00215

was included in the dataset of the CMap tool and a gene-expression profile of spironolactone treatment was available from three cancer cell lines: MCF7 breast cancer, PC-3 adenocarcinoma, and HL60 leukemia. Using the spironolactone expression profile as a query in the CMap tool resulted in a list of small molecules with related expression profiles, which can be used to point towards a possible mechanism. Search of the literature regarding the top five ranking results, trichostatin A (TSA), chlorocyclizine, halcinonide, nystatin, and santonin (Fig. 5c), suggested that three of these molecules, chlorocyclizine, halcinonide, and nystatin, play different roles that could all be attributed, directly or indirectly, to the canonical role of spironolactone as an antagonist of MR (Supplementary Fig. S4B). Interestingly, we found a role in apoptosis for the remaining two molecules, TSA and santonin. The histone deacetylase inhibitor TSA was ranked at the top (Fig. 5c), with a modest specificity score of 0.5213. This is probably due to the fact that a histone deacetylase inhibitor has many roles and affects numerous pathways. Importantly, TSA was shown to promote cancer cell apoptosis [24, 25]. On the other hand, santonin,

◀ **Fig. 5** Spironolactone does not act through aldosterone antagonism and induces apoptosis in cancer and CSCs. **a** CSCL cells were treated with the indicated concentrations of the aldosterone antagonist, eplerenone, or with DMSO (Control) for 1 h prior to 1 h treatment, when indicated, with phleomycin. Cells were recovered in an appropriate fresh medium containing DMSO or eplerenone, at the indicated concentrations, for 96 h and then fixed and stained with methylene blue. Relative growth was quantified by reading at 620 nm in a microplate reader. Results are normalized to control amounts and are shown as the average of six technical repeats of a representative experiment. SE bars are shown. **b** CSCL cells were treated for 6 h with 100 nM aldosterone; addition of 20 μM spironolactone or 20 μM eplerenone is indicated. mRNA was extracted and cDNA was prepared. GADD45β levels were determined by RT-PCR. Average values from three repeats normalized to control. SE bars are shown. **c** Top hit results for query "spironolactone" (twofold change) as shown in 'permuted results table' in CMap computational tool. 'Mean' is the arithmetic mean of the connectivity scores. 'Enrichment' is a measure of the correlation strength; positive enrichment, expression pattern is similar; negative enrichment, opposite effect; high enrichment score, tighter correlation. 'Specificity' is an estimate of the uniqueness of the connectivity. High specificity extent of connectivity is unexceptional and/or the molecule involved has multiple biological effects. **d** Western blot for cleaved PARP of cells treated with an equivalent amount of DMSO (Control spironolacton (S) and Control eplerenone (E)), 50 μM spironolactone (Spiro), 100 μM eplerenone or 2.5 μM of the protein kinase inhibitor staurosporine (STS) for 24 h. GAPDH as a control. **e** Relative apoptosis levels represented by the ratio of cleaved PARP after indicated treatments. Bands of WB presented in (**d**) were quantified using ImageJ and values were normalized to GAPDH and then to the relevant control

which was ranked fifth in the search, was highly specific (a specificity score of 0), yet relatively poorly enriched (an enrichment score of 0.816; Fig. 5c). This drug expels parasitic worms from the body and was reported to cause G2/M arrest and apoptosis in cancer cells [26]. Since eplerenone did not induce a similar effect to that of spironolactone, we hypothesized that the growth inhibition effect of spironolactone was due to the activation of apoptosis in cancer cells and CSCs. To test our hypothesis, we treated cancer U2OS and CSCL cells with spironolactone. As a positive control for the induction of apoptosis, cells were treated with staurosporine (STS), a potent protein kinase inhibitor, known to induce apoptosis [27]. Apoptosis was detected by the presence of the cleaved form of poly(ADP-ribose) polymerase (PARP), a marker of apoptosis [28]. Treating U2OS cells with STS resulted in the cleavage of the 116-kDa PARP band, leading to the appearance of the cleaved PARP fragment of 89 kDa (Fig. 5d). When treating U2OS cells with spironolactone, the cleaved PARP fragment was also displayed, although at a lower intensity, compared to STS (Fig. 5d, e). In CSCL cells, the effect of spironolactone was even stronger; treatment with spironolactone resulted in higher levels of cleaved PARP when compared to the control STS treatment (Fig. 5d, e). Notably, treating the cells with eplerenone did not induce apoptosis in CSCL cells (Fig. 5d, e). Taken together, we conclude that spironolactone may act on cancer cells and CSCs to inhibit their growth through apoptosis.

Spironolactone reduces CSC content in vivo

To establish the possible role of spironolactone as an anticancer reagent it was important to test its effect in vivo. Previous experiments in mice showed the ability of spironolactone to shrink the volume of tumors originated from different cell lines [6, 8]. We used the CSCL system, in which the tumors formed can be assessed not only in terms of the final tumor volume but also in terms of CSC content (measured by the fraction of $SSEA1^+$ cells). We injected the transformed cells, from which the CSCL cells are generated [16], into NOD-SCID mice. To provide a clinical relevant setup, in which treatment begins only after tumors are formed, we allowed a period for tumor growth before treating the mice. In order to compare the effect of spironolactone to available chemotherapies, we tested in parallel the effect of cisplatin. Both cisplatin and spironolactone treatments reduced tumor weight (Fig. 6a). In light of the CSC theory, stating that a small population of chemoresistant cells are not affected by the treatment and are able to eventually reinitiate tumor growth and or metastasize [14], we examined the CSC content in tumors following different treatments. The CSC content was assessed as the percent of SSEA1-positive cells in the tumor; an apparent reduction in CSC content was seen for both spironolactone and cisplatin treatments compared to control (Fig. 6b). However, in contrast to the trend viewed in tumor weight, in which tumors extracted from mice treated with cisplatin are slightly smaller than those extracted from mice treated with spironolactone (Fig. 6a), CSC content of tumors derived from mice treated with spironolactone was slightly lower than those derived from cisplatin-treated mice (Fig. 6b). Analysis of the correlation between tumor size and CSC content highlighted a striking fact; both in control and cisplatin-treated mice, CSC content was higher as a function of a smaller tumor weight (Fig. 6c). This is in contrast to spironolactone treatment, which showed the opposite correlation of increasingly lower CSC content as tumor weight decreases (Fig. 6c). This correlation may point to a fundamental and dangerous phenomenon in cancer therapy in which treatment that is not specifically targeted to the CSC subpopulation can shrink the tumor but in the process, a selection in favor of the CSCs is occurring, which can eventually drive tumor regrowth. It is important to note that when mice were sacrificed at the end of the treatment, 2 out of 16 mice treated with spironolactone had no visible tumors whatsoever.

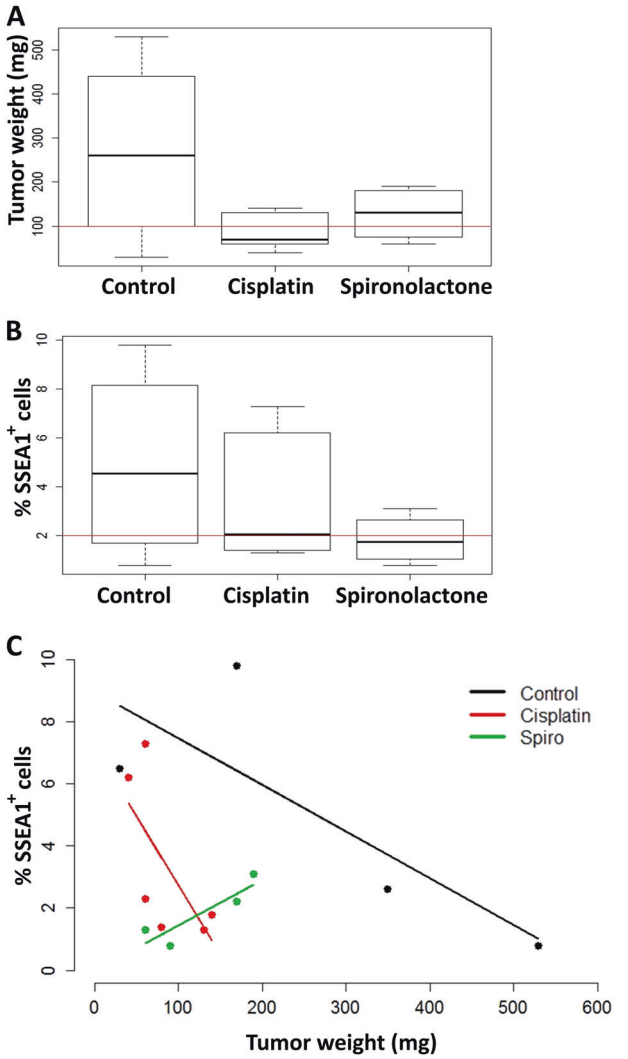

Fig. 6 Spironolactone effect on tumor growth and cancer stem cell content. NOD/SCID mice were injected with $1 \times 10\text{^}4$ transformed cells ($+ 1 \times 10\text{^}5$ immortalized cells) and tumors were allowed to develop for 3 weeks. Mice were treated IP for three consecutive weeks either with 3 mg/kg cisplatin once a week or 50 mg/kg spironolactone (Spiro) twice a week, or control (corn oil : PBS). Tumors were harvested, weighed (**a**) and % $SSEA1^+$ cells were determined by flow cytometry (**b**). Linear modeling of the correlation between tumor size and CSC content was analyzed by R software (**c**). Tumors: Spiro and Control, 4n; cisplatin, 6n

Discussion

In this work, we found that the antihypertensive drug spironolactone can inhibit the growth of cancer and CSCs, while sparing the healthy cells. Moreover, we found that spironolactone reduces tumor size and CSC content in mice. The ability of a chemical or potential drug to act in a differential manner on different targets holds the potential of minimizing side effects and enhancing the efficacy of the treatment.

This work is an example for the benefit of combination therapy between DNA-damaging agents and inhibitors of DNA-repair pathways [29]. Our results suggest that in cancer cells, a combination of the DNA-damaging agent, such as phleomycin or cisplatin, together with spironolactone has a larger effect than using any of those alone, especially lower doses of spironolactone treatment on cancer cells. However, a close examination of the combined treatment on healthy cells or CSCs reveals that spironolactone treatment alone may actually be more beneficial. In the case of CSCL cells, DNA-damaging agents do not affect growth whatsoever, making the treatment redundant. In healthy cells however, phleomycin has some inhibiting effect on growth, which may be deleterious. Treatment with spironolactone only seems not to harm healthy cells, and not at the expense of treating CSCs. This is especially important since the original discovery of anticancer drugs was done based on their effect on cancer cells only, but today the toxic side effects, such as nephrotoxicity of cisplatin or cardiomyopathy of doxorubicin, are known [30]. Special attention is therefore given to drugs that are used in a context other than cancer and have the potential of being safer drugs. Another advantage of spironolactone in terms of safety is reflected in our findings that spironolactone did not induce DNA damage in cells. Spironolactone exerts its effect in the later stages of DDR resulting in delayed DNA repair in cancer and CSCs, specifically, as well as apoptosis induction.

The differential response that spironolactone elicits in terms of DDR on the different cell types can explain the complex effect of spironolactone on growth. This led us to propose a model that explains the differential effect of spironolactone on different cell types based on the DDR state of the treated cells (Fig. 7). The genome of cancer cells is extremely unstable and carries out alternative expression patterns that enhance replication and transcription driving to replication stress, replication fork slowing, and accumulation of DNA damage [31]. Therefore, interfering with the DDR of cancer cells by use of spironolactone, even without an external induction of DNA damage, may lead to the exhibited growth inhibition in cancer cells. Healthy cells, on the other hand, have an intact genome and a functional DDR, which can explain why spironolactone does not harm those cells, in contrast to cancer or CSCs. CSCs displayed a striking sensitivity to spironolactone, resulting in a remarkable growth inhibition. In terms of DDR, we observed that CSLC cells are both resistant to DNA-damaging agents and display basal levels of damage reflected directly by longer comet tails. According to the gradual dependence on intact DDR it would be expected that CSC sensitivity to DNA-damaging agents would be high, but due to CSC resistance, which is a result of various reasons, among them the expression of drug efflux pumps,

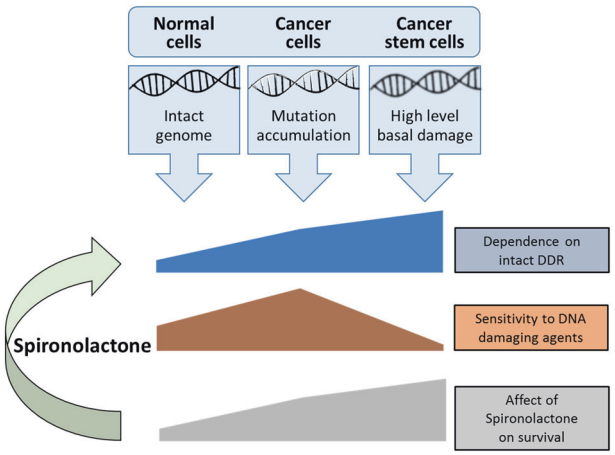

Fig. 7 Proposed model: differential effect of spironolactone on different cell types is dependent on DDR state and genomic integrity. Cancer cells, unlike healthy cells, suffer from accumulated mutations that may affect the DDR. Therefore, cancer cells, compared to healthy cells, have a higher dependence on the intact activity of the remaining DDR. In addition to cancer cell traits, CSCs display constant levels of basal damage indicating an ongoing dependence on DDR, which may be reflected in the reported high levels of DDR in those cells. According to the gradual dependence on intact DDR it would be expected that sensitivity to DNA-damaging agents would display a similar pattern in cancer cells. However, due to CSC resistance (for various reasons, among them the expression of drug efflux pumps), the CSCs are not sensitive to these chemotherapeutic drugs. Because spironolactone affects DDR, the resistance of CSCs is bypassed and the gradual pattern of dependence on the intact DDR plays the major role, resulting in growth inhibition of cancer and CSCs while sparing the healthy cells

they are not sensitive to these chemotherapeutic drugs. Because spironolactone affects DDR, the resistance of CSCs is bypassed and the gradual pattern of dependence on intact DDR plays the major role, resulting in growth inhibition of CSCs.

The resistance of CSCs to DNA-damaging agents is well documented and is attributed in part to a highly active DDR [32–35]. However, we found both by analyzing comet tails as well as γH2AX levels and focus formation that CSCL cells have a high basal level of damage and damage signaling, regardless of DNA-damage induction. This may seem to stand in contradiction to the current understanding of a highly active DDR in CSCs, which responds to damage. However, a close examination of the data presented in the literature actually provides evidence supporting the basal activity of DDR in CSCs, without DNA-damage induction. For instance, phosphorylation of proteins involved in DDR, such as Chk1, Chk2, Rad17, p38, and AKT, was observed in CSCs even without treatment with DNA-damaging agents [32, 35]. Our findings together with the data that we retrieved from the literature support the notion that CSCs possess a highly active DDR, but even more so, the DDR in CSCs seems to be "on call", active all the time on a basal level. It is not only an enhanced DDR, but rather a primed state ready to tackle any damage in sight, enabling immediate attending to any damage occurring. This trait holds an obvious advantage to a stem cell by protecting the genetic material passed on to all progeny, but in CSCs this is a lethal weapon contributing to resistance. Exploiting the special state of DDR in CSCs presents an opportunity to target this ultrasensitive system. Interfering with the essential DDR activity carries the potential to damage the CSCs even without any additional DNA damage.

The special contribution that spironolactone may provide in treating cancer is demonstrated in our in vivo experiments. Although treatment with the common chemotherapy cisplatin was more efficient than spironolactone in slowing the rate of tumor growth, it resulted in a higher percent of $SSEA1^{+}$ cells within the tumors, suggesting a selection process in favor of the hazardous CSC population. Spironolactone, on the other hand, had the ability both to slow down the rate of growth compared to control treatment as well as to reduce the CSC proportion relative to control and cisplatin treatments. It is important to note that cisplatin treatment presents a severe side effect of nephrotoxicity [36]. It could therefore be beneficial to combine cisplatin treatment for a short period of time with a long-term spironolactone treatment, thus maximizing the therapeutic effect of each of the drugs while minimizing the side effects. Supporting our study is a recent study that demonstrated a lower risk of urinary tract cancers in patients with hypertension who were treated with spironolactone [37]. However, in the context of cancer therapy and clinical relevance, the path of course is not fully paved. In the process of the future transfer of spironolactone to the clinic, several obstacles should be considered. For instance, spironolactone dosage in our experiments is higher by about two orders of magnitude than the doses, monitored in serum concentrations, that patients are currently being treated with it for heart failure conditions [38]. Yet it is far from the intraperitoneal LD50 in mice [39]. The stability state of spironolactone and properties of its metabolites should be taken into account as well and should defiantly be addressed in future works. Nevertheless, our findings are promising and hold a potential for the future use of spironolactone in cancer treatment, specifically in the elimination of CSCs.

Methods

Cell lines and media

U2OS, HeLa, RPE1 hTERT, FSE hTERT, BJ hTERT, and BJ cells were cultured in Dulbecco's modified eagle's medium (Biological Industries, BI) supplemented with 10% fetal bovine serum (FBS) (BI), 20 mM L-glutamine (BI),

500 units/ml penicillin (BI), and 0.5 mg/ml streptomycin (BI). Cells were detached with trypsin (BI).

CSCL and original immortalized cells were additionally supplemented with 1% MEM Eagle (BI) and 5% FBS (BI). Cells were detached with trypsin (BI).

SLGCs were cultured in a neurobasal medium (Difco) supplemented with 20% v/v BIT serum replacement (Stem Cell Technologies), 2 mM L-glutamine, 50 μg/ml penicillin/streptomycin, and 20 ng/μl basic fibroblast growth factor (FG) and epidermal growth factor (EGF) (Peprotech). Cells were dissociated with accutase (Sigma-Aldrich).

Hematopietic stem cells from samples of cord blood were obtained according to procedures approved by the institutional review board of Tel Aviv Sourasky Medical Centre and Tel Aviv University, Israel. Lineage depletion and CD34 + cell enrichment of cord blood samples were achieved by a negative selection with the EasySep system according to the manufacturer's protocol (Stem Cell Technologies). CD34 + cells were grown in Iscove's Modified Dulbecco's Medium (IMDM), 10% FBS supplemented with Fms-related tyrosine kinase 3 ligand (FLT3L) (50 ng/ml), thyroperoxidase (TPO) (20 ng/ml), Stem cell factor (SCF) (50 ng/ml), and IL-6 (10 ng/ml).

All cells were maintained in a humidified incubator at 37 °C and with 5% CO_2.

Immunofluorescence

U2OS, BJ hTERT and CSCL cells were grown on cover slips placed in six-well tissue culture dishes. The cells were incubated for 1h with 40 μM spironolactone (Sigma-Aldrich) or an equivalent volume of DMSO (Merck Millipore) for control. DNA damage was induced with phleomycin (10 μg/ml, Invivogen) for 1 h and then replaced with media containing spironolactone or DMSO for 6 h. The cells were fixed with 4% paraformaldehyde and permeabilized with 0.5% Triton X-100. The cells were incubated for 2 h with mouse anti-phospho-Histone H2A.X, Ser139 (γH2AX, Merck Millipore; 05–636, 1:300), washed three times in phosphate-buffered saline (PBS), and incubated for 1 h with Dylight 488 (Jackson Immunoresearch Laboratories; 211-482-171, 1:700). The cells were washed three times, stained with 4′,6-diamidino-2-phenylindole (DAPI; MP Biomedicals) and mounted on glass slides (DakoCytomation). γH2AX foci were imaged by a Olympus IX81 fluorescence microscope with a 60 × oil objective. At least 50 cells were analyzed for each treatment.

γH2AX in flow cytometry

U2OS, BJ hTERT, and CSCL cells were grown in six-well tissue culture dishes. Cells were treated for 1 h with 40 μM spironolactone (Sigma-Aldrich) or a DMSO equivalent volume (Merck Millipore) for control. DNA damage was induced with 15 μg/ml phleomycin (Invivogen) for 1 h and then replaced with media containing spironolactone or DMSO for 1, 6, or 16h. Cells were detached from the wells with trypsin, pelleted in Eppendorf tubes (1200 RCF, 3 min, 4 °C), and resuspended in 4% paraformaldehyde for 30 min on ice. Cells were pelleted again and re-suspended in FACS buffer (PBS, 1% fetal calf serum (FCS), 0.05% sodium azide) and kept overnight at 4 °C. The following day cells were pelleted, washed twice in saponin solution (0.1% saponin (Sigma-Aldrich) in FACS buffer) to perforate the membrane, and resuspended in saponin solution containing mouse anti-phospho-Histone H2A.X, Ser139, (γH2AX, Merck Millipore; 05–636, 1:500) for 30 min on ice. Staining was terminated by the addition of 1 ml saponin solution followed by three washes as described above. Cells were incubated with saponin solution containing goat anti-mouse DyLight 488 (Jackson Immunoresearch Laboratories; 211-482-171, 1:1000) for 30 min on ice and washed again three times. Cells were finally suspended in FACS buffer. Cells were read for each sample with the green (488 nm) laser of FACSAria III (BD Biosciences) and FACSDiva (version 7) program. Thirty thousand cells were analyzed for each experiment, and data are shown as average of 2–3 repeats for each condition.

Comet assay

U2OS and CSCL cells were grown in six-well tissue culture dishes. The cells were incubated with 40 μM spironolactone (Sigma-Aldrich) or an equivalent volume of DMSO (Merck) for control for 1–5h. DNA damage was induced with phleomycin (Invivogen; 10 μg/ml, 1 h) or with an exposure to UV (11.3 mJ/cm^2, 4 h recovery to allow DSB formation) and then replaced with media containing spironolactone or DMSO. During UV treatment, the mediium was substituted by PBS to reduce interference with irradiation and then immediately replaced after irradiation. Cells were collected (1200 rpm, 3 min, room temperature (RT)) and embedded in soft agar on glass slides, followed by lysis and fixation (TREVIGEN, kit 18008738443). Glass slides were placed in a gel electrophoresis apparatus and run under neutral electrophoresis conditions according to kit instructions. Nuclei were stained with DAPI (MP Biomedicals), and comet tails were imaged by an Olympus IX81 fluorescence microscope and analyzed with the "open comet" software. Seventy to hundred nuclei were analyzed for each condition.

Growth assays

Cells were plated in a 96-well plate in the indicated densities (HeLa, 750 cells/well; U2OS and CSCL, 1000 cells/

well; immortalized fibroblasts, 2000 cells/well; RPE1 hTERT, 4000 cells/well; BJ hTERT and FSE hTERT, 6000 cells/well, and BJ, 8000 cells/well). Twenty four hours after seeding, the cells were treated for 1 h with media containing spironolactone (Sigma-Aldrich) or eplerenone (Cayman) at indicated concentrations. For control, equivalent volumes of DMSO were added. DNA damage was induced with the addition of phleomycin (Invivogen, 15 μg/ml) or cisplatin (Enzo Life Science), for 1 h, and then replaced with a fresh medium containing spironolactone, eplerenone, or DMSO in the original concentrations. After 96 h, the cells were fixed with 0.25% glutaraldehyde and dyed with methylene blue (Sigma-Aldrich) dissolved in 0.1 M boric acid. Color was extracted by 0.1 M Hcl, and the intensity was quantified by light absorbance at 620 nm with a plate reader device (Biotec). Values were shown as the average of three experiments, six technical repeats each or as the average of 3–6 technical repeats of a representative experiment, as indicated in relevant figure legends.

SLGCs were grown in 12-well tissue culture dishes. Cells were treated with 15 μg/ml phleomycin (Invivogen) for 1 h and washed. Cells were grown in the presence of an indicated concentration of spironolactone (Sigma-Aldrich) or an equivalent volume of DMSO as control for a total of 8 days (on day 4, a fresh medium was supplied). Neurosphere morphology was visualized under a light microscope and representative fields were captured. In parallel, 100 μl from each condition were transferred to a 96-well culture dish (in duplicate) and stained with 1:10 WST1 Cell Proliferation Reagent (Roch). Intensity was quantified by light absorbance at 450 nm with a plate reader device (Biotec).

Hematopoietic stem cells were seeded at a density of 1 × 105 cells/ml. Colony forming assay was performed in MethoCult™ H4434 Classic with recombinant cytokines and EPO (Stem Cell Technologies, Canada). Colonies were counted after 12–14 days of incubation.

RT-PCR

CSCL cells were treated for 6 h with 100 nM aldosterone (Arcos Organics) and 20 μM spironolactone (Sigma-Aldrich) or 20 μM eplerenone (Cayman). mRNA was extracted (EZ-RNA, BI) from the collected cells. The extracted RNA was reverse transcribed according to the manufacturer's instructions of the High-Capacity cDNA Reverse Transcription Kits (Applied Biosystems). Real-time quantitative RT-PCR based on the SYBR Green methodology was done (three repeats) with the StepOnePlus™ Real-Time PCR System (Rhenium). Gene expression was calculated relatively to the control gene GAPDH.

Primer sequences used are *GAPDH*: forward primer sequence 5′−3′: AGCCACATCGCTCAGACACC, reverse primer sequence 5′−3′: GTATCTAGCGCCAGCATCG; *GADD45β*: forward primer sequence 5′−3′: CATTGTC TCCTGGTCACGAA, reverse primer sequence 5′−3′: CATTGTCTCCTGGTCACGAA.

Apoptosis analysis

U2OS and CSCL cells were grown in six-well tissue culture dishes. Fifty micromolar of spironolactone (Sigma-Aldrich), 100 μM eplerenone (Cayman) or 2.5 μM STS were added for 24 h. Cells were collected and lysed with 2 × loading sample buffer (containing sodium dodecyl sulfate and dithiothreitol). Samples were run on sodium dodecyl sulfate-polyacrylamide gel and blotted onto nitrocellulose membrane. The membrane was incubated with rabbit anti-Poly(ADP-ribose) polymerase (PARP, Cell signaling; #9542, 1:1000) and mouse anti-GAPDH (Abcam; ab8245, 1:10,000) antibodies. Signal was detected on a film after exposing the membranes to EZ-ECL reagents (BI).

In vivo mice experiment

NOD-SCID 5-week-old male mice were injected with 1 × 10^4 transformed cells (+ 1 × 10^5 immortalized cells) and tumors were allowed to develop for 3 weeks. Mice were treated intraperitoneally (IP) for three consecutive weeks either with 3 mg/kg cisplatin once a week (Wednesday) or 50 mg/kg spironolactone twice a week (Sunday and Wednesday) or control (corn oil:PBS).

Tumors were harvested from culled mice and weighed (four tumors for control and spironolactone and six for cisplatin). Tumors were minced and dissociated in Dulbecco's modified eagle's medium 10% FCS containing 2 mg/ml collagenase IV (Worthington), hyaluronidase 1:100 (Sigma-Aldrich), and DNase 1:1000 (Roche) for 1 h while shaking at 180 rpm, 37 °C, followed by intensive pipetation. Cells were centrifuged at 300 g, 5 min, RT, and the pellet was washed twice with 2% FCS in PBS. Cells were treated for 2 min with 0.8% NH_4Cl, washed again with 2% FCS in PBS, and pelleted at 300 g, 5 min, RT. For single-cell suspension, cells were passed through a 70 μm cell strainer. Cells were counted and frozen in 10% DMSO in FCS. Dissociated tumor cells were incubated for 40 min at 4 °C in sort buffer (1% BSA, 1% pen/strep, 2 mM Ethylenediaminetetraacetic acid (EDTA), 15 mM - 4-(2-Hydroxyethyl) piperazine-1-ethanesulfonic acid (HEPES) in PBS) containing anti-human/mouse SSEA-1–Alexa 647 (eBiosciences; 50-8813-42, 1:20), anti-human CD166–PE (eBiosciences; 559263, 1:20), anti-mouse MHC-FITC (eBiosciences; 11-5998-82, 1:300) antibodies. Cells were washed twice with sort duffer and centrifuged at 300 g, 5 min. Incubation with sort buffer containing DAPI (MP Biomedicals; 1:5000) for 10 min at RT was followed immediately. $SSEA1^+/CD166^+/MHC^-$ cells were detected

using the FACSAria III (BD Biosciences) and FACSDiva (version 7) program.

The joint ethics committee (IACUC) of the Hebrew University and Hadassah Medical Center approved the study protocol for animal welfare. The Hebrew University is an AAALAC International accredited institute. All animal experiments were conducted in accordance with the Hebrew University's animal committee, ethical approval number IACUC:NS-09-15102-4).

Acknowledgements We thank the members of our laboratory for supportive discussions and lab assistance: Paola Scaffidi and Thomas Mortimer for helping with the CSCL cell system; Christel Herold-Mende for providing us SLGCs; Yuval Dor and Elad Horwitz for comet assay assistance; Dan Sarni for software advice; Batsheva Kerem for providing healthy cells; Adva Biran and Uri Ben-David for CSC advice; Nissim Benvenisty for helpful advice and Evi Soutoglou for providing anti-XPB antibodies.

Funding This work was supported by grant 1353/12 from the Israel Science Foundation and grant 20171152 from the Israel Cancer Association, with the generous assistance of Nancy and Peter Brown through the ICA USA to MG, and by grant 1140/17 from the Israel Science Foundation and CA180 from the DKFZ-MOST Collaboration to EM.

Compliance with ethical standards

Conflict of interest The authors declare that they have no conflict of interest.

References

1. Rajanna A. Novel approach to target cancer stem cells for therapy. Med Hypotheses. 2016;88:83–5.
2. Hanahan D, Weinberg RA. Hallmarks of cancer: the next generation. Cell. 2011;144:646–74.
3. Ferguson LR, Chen H, Collins AR, Connell M, Damia G, Dasgupta S, et al. Genomic instability in human cancer: Molecular insights and opportunities for therapeutic attack and prevention through diet and nutrition. Semin Cancer Biol. 2015;35:S5–24.
4. Harper JW, Elledge SJ. The DNA damage response: ten years after. Mol Cell. 2007;28:739–45.
5. Gavande NS, VanderVere-Carozza PS, Hinshaw HD, Jalal SI, Sears CR, Pawelczak KS, et al. DNA repair targeted therapy: The past or future of cancer treatment? Pharmacol Ther. 2016;160:65–83.
6. Shahar OD, Kalousi A, Eini L, Fisher B, Weiss A, Darr J, et al. A high-throughput chemical screen with FDA approved drugs reveals that the antihypertensive drug Spironolactone impairs cancer cell survival by inhibiting homology directed repair. Nucleic Acids Res. 2014;42:5689–701.
7. Alekseev S, Ayadi M, Brino L, Egly JM, Larsen AK, Coin F. A small molecule screen identifies an inhibitor of DNA repair inducing the degradation of TFIIH and the chemosensitization of tumor cells to platinum. Chem Biol. 2014;21:398–407.
8. Leung WH, Vong QP, Lin W, Janke L, Chen T, Leung W. Modulation of NKG2D ligand expression and metastasis in tumors by spironolactone via RXRγ activation. J Exp Med. 2013;210:2675–92.
9. Struthers A, Krum H, Williams GH. A comparison of the aldosterone-blocking agents eplerenone and spironolactone. Clin Cardiol. 2008;31:153–8.
10. Funder JW. Mineralocorticoid receptor antagonists: emerging roles in cardiovascular medicine. Integr Blood Press Control. 2013;6:129–38.
11. Baker M. Cancer stem cells, becoming common. Nat. Reports Stem Cells. 2008. https://doi.org/10.1038/stemcells.2008.153
12. Bandhavkar S. Cancer stem cells: A metastasizing menace!. Cancer Med. 2016;5:649–55.
13. Shaked Y. Balancing efficacy of and host immune responses to cancer therapy: the yin and yang effects. Nat Rev Clin Oncol. 2016;13:611–26.
14. Clarke MF. Self-renewal and solid-tumor stem cells. Biol Blood Marrow Transplant. 2005;11:14–6.
15. Peitzsch C, Tyutyunnykova A, Pantel K, Dubrovska A. Cancer stem cells: The root of tumor recurrence and metastases. Semin Cancer Biol. 2017;44:10–24.
16. Scaffidi P, Misteli T. In vitro generation of human cells with cancer stem cell properties. Nat Cell Biol. 2011;13:1051–61.
17. Campos B, Wan F, Farhadi M, Ernst A, Zeppernick F, Tagscherer KE, et al. Differentiation therapy exerts antitumor effects on stem-like glioma cells. Clin Cancer Res. 2010;16:2715–28.
18. Torres CM, Torres CM, Biran A, Burney MJ, Patel H, Henser-Brownhill T, et al. The linker histone H1.0 generates epigenetic and functional intratumor heterogeneity. Science. 2016;353:aaf1644–1aaf1644-11.
19. Singh SK, Hawkins C, Clarke ID, Squire JA, Bayani J, Hide T, et al. Identification of human brain tumour initiating cells. Nature. 2004;432:396–401.
20. Dictus C, Tronnier V, Unterberg A, Herold-Mende C. Comparative analysis of in vitro conditions for rat adult neural progenitor cells. J Neurosci Methods. 2007;161:250–8.
21. Biechonski S, Yassin M, Milyavsky M. DNA-damage response in hematopoietic stem cells: An evolutionary trade-off between blood regeneration and leukemia suppression. Carcinogenesis. 2017;38:367–77.
22. Chadwick JA, Lowe J, Shaw JJ, Guttridge DC, Gomez-Sanchez CE, Gomez-Sanchez EP, et al. Mineralocorticoid receptors are present in skeletal muscle and represent a potential therapeutic target. FASEB J. 2015;29:4544–54.
23. Lamb J. The Connectivity Map: a new tool for biomedical research. Nat Rev Cancer. 2007;7:54–60.
24. Taghiyev AF, Guseva NV, Sturm MT, Rokhlin OW, Cohen MB. Trichostatin A (TSA) sensitizes the human prostatic cancer cell line DU145 to death receptor ligands treatment. Cancer Biol Ther. 2005;4:382–90.
25. Choi YH. Induction of apoptosis by trichostatin A, a histone deacetylase inhibitor, is associated with inhibition of cyclooxygenase-2 activity in human non-small cell lung cancer cells. Int J Oncol. 2005;27:473–9.
26. Ferreira JRO, Cavalcanti BC, da Costa PM, de Arantes FF, de Alvarenga ES, Maltha CR, et al. Induction of G_2/M arrest, caspase activation and apoptosis by α-santonin derivatives in HL-60 cells. Toxicol Vitr. 2013;27:1458–66.
27. Belmokhtar CA, Hillion J, Ségal-Bendirdjian E. Staurosporine induces apoptosis through both caspase-dependent and caspase-independent mechanisms. Oncogene. 2001;20:3354–62.
28. Oliver FJ, de la Rubia G, Rolli V, Ruiz-Ruiz MC, de Murcia G, Murcia JM. Importance of poly(ADP-ribose) polymerase and its

cleavage in apoptosis. Lesson from an uncleavable mutant. J Biol Chem. 1998;273:33533–9.
29. Helleday T, Petermann E, Lundin C, Hodgson B, Sharma RA. DNA repair pathways as targets for cancer therapy. Nat Rev Cancer. 2008;8:193–204.
30. Cheung-Ong K, Giaever G, Nislow C. DNA-damaging agents in cancer chemotherapy: serendipity and chemical biology. Chem Biol. 2013;20:648–59.
31. Kotsantis P, Silva LM, Irmscher S, Jones RM, Folkes L, Gromak N. et al. Increased global transcription activity as a mechanism of replication stress in cancer. Nat Commun. 2016;7:13087.
32. Bao S, Wu Q, McLendon RE, Hao Y, Shi Q, Hjelmeland AB. et al. Glioma stem cells promote radioresistance by preferential activation of the DNA damage response. Nature. 2006;444:756–60.
33. Louka M, Boutou E, Bakou V, Pappa V, Georgoulis A, Stürzbecher HW et al. DNA damage response/repair in cancerstem cells — potential vs. controversies. In: Advances in DNA Repair. 2015. https://doi.org/10.5772/61355
34. Chen Y, Li D, Wang D, Liu X, Yin N, Song Y, et al. Quiescence and attenuated DNA damage response promote survival of esophageal cancer stem cells. J Cell Biochem. 2012;113:3643–52.
35. Chang CH, Zhang M, Rajapakshe K, Coarfa C, Edwards D, Huang S, et al. Mammary stem cells and tumor-initiating cells are more resistant to apoptosis and exhibit increased DNA repair activity in response to DNA damage. Stem Cell Rep. 2015;5:378–91.
36. Yao X, Panichpisal K, Kurtzman N, Nugent K. Cisplatin nephrotoxicity: a review. Am J Med Sci. 2007;334:115–24.
37. Chuang Y, Yu MC, Huang ST, Yang CK, Chen CH, Lo YC, et al. Spironolactone and the risk of urinary tract cancer in patients with hypertension. J Hypertens. 2017;35:170–7.
38. Gardiner P, Schrode K, Quinlan D, Martin BK, Boreham DR, Rogers MS, et al. Spironolactone metabolism: steady-state serum levels of the sulfur-containing metabolites. J Clin Pharmacol. 1989;29:342–7.
39. Lumb G, Newberne P, Rust JH, Wagner B. Effects in animals of chronic administration of spironolactone--a review. J Environ Pathol Toxicol. 1978;1:641–60.